Carbohydrate Polymers 117 (2015) 687–693

Contents lists available at ScienceDirect

Carbohydrate Polymers

journal homepage: www.elsevier.com/locate/carbpol

Pectin/lysozyme bilayers layer-by-layer deposited cellulose nanofibrous mats for antibacterial application

Tingting Zhang[a,b,1], Panghu Zhou[c,1], Yingfei Zhan[a], Xiaowen Shi[a], Jinyou Lin[d], Yumin Du[a], Xiuhong Li[d,**], Hongbing Deng[a,b,*]

[a] Department of Environmental Science, Hubei Key Lab of Biomass Resource Chemistry and Environmental Biotechnology, School of Resource and Environmental Science, Wuhan University, Wuhan 430079, China
[b] College of Food Science and Technology, Huazhong Agricultural University, No. 1 Shizishan Road, Wuhan 430070, China
[c] Department of Orthopedics, Renmin Hospital of Wuhan University, Wuhan 430060, China
[d] Shanghai Institute of Applied Physics, Chinese Academy of Sciences, Shanghai 201204, China

ARTICLE INFO

Article history:
Received 19 July 2014
Received in revised form 16 October 2014
Accepted 23 October 2014
Available online 30 October 2014

Keywords:
Nanofibrous mats
Pectin
Lysozyme
Layer-by-layer
Bacterial inhibition ability

ABSTRACT

Positively charged lysozyme (LZ) and negatively charged pectin, were alternately deposited on the surface of the cellulose nanofibrous mats by layer-by-layer (LBL) self-assembly technique. Scanning electron microscopy images showed that the nanofibers were orderly and compactly arrayed after LBL. Besides, as the number of LZ/pectin bilayers increased, the average diameter of nanofibers increased. LZ has assembled on the cellulose mats successfully, which was confirmed by X-ray photoelectron spectroscopy analysis. Thermal gravimetric analysis results showed that the thermal properties of LZ/pectin films coated mats was better than that of the unmodified cellulose mats. Importantly, the results of the bacterial inhibition test for LBL structured mats and cellulose mats indicated that the nanofibrous mats coated by 10.5 LZ/pectin bilayers (with LZ on the outmost layer) possessed the strongest inhibitory effect against both *Escherichia coli* and *Staphylococcus aureus*.

1. Introduction

Layer-by-layer (LBL) self-assembly technique, introduced by Decher, Hong, and Schmitt (1992), has became one of the most frequently utilized processes for preparing functional ultra-thin films on the surface of various templates, including flat plate (Marcus, Anderson, & Quake, 2006), microspheres (Yu, Yu, Liu, & Mann, 2007), nanoparticles (Ding & Gin, 2000), nanofibers (Deng et al., 2013), etc. And nanofibrous mats attracted intensive attentions because they possessed some unique characteristics such as the ultra-thin fiber diameter, small pore size, high specific surface area and three-dimensional (3D) structure (Deng et al., 2013, 2011b). Various methods for fabricating nanofibers including electrospinning, phase separation, and template synthesis have been used, and electrospinning is considered as a simple and efficient method because it is straightforward, versatile, cost effective and scalable (Hartgerink, Beniash, & Stupp, 2001; Zhang, Venugopal, Huang, Lim, & Ramakrishna, 2005). Fibers could be applied to enhance the performance in various areas like wound healing (Noh et al., 2006), sensors (Wang et al., 2011), tissue engineering (Yang, Chen, & Wang, 2009), drug delivery (Hou et al., 2011) and antibacterial applications (Deng et al., 2011b).

Actually, the pure nanofibrous mats hardly showed antimicrobial property and the electrospinning of antimicrobial agents was still a big challenge. But by using LBL self-assembly technique, antimicrobial agents can be used to produce functional LBL structured composite films. Driven by electrostatic force, antimicrobial agents with opposite charges are able to alternately assemble onto the surface of nanofibers, such as cellulose acetate (CA) nanofibers, polylactic acid nanofibers, poly acetyl imine nanofibers, etc. Compared to synthetic antimicrobial agents, the natural antimicrobial agents has many unique properties such as biodegradability and nontoxicity. Natural antimicrobial agents, such as lysozyme (LZ), pectin, chitosan and alginic acid, are great candidates for deposition materials to prepare LBL structured films with improved

* Corresponding authors at: Wuhan University, Department of Environmental Science, Hubei Key Lab of Biomass Resource Chemistry and Environmental Biotechnology, School of Resource and Environmental Science, No.129 Luoyu Road, Wuhan 430079, China. Tel.: +86 27 68778501; fax: +86 27 68778501.
** Corresponding authors at: Shanghai Institute of Applied Physics, Chinese Academy of Sciences, Shanghai 201204, China. Tel.: +86 21 33933219; fax: +86 21 33933219.
E-mail addresses: lixiuhong@sinap.ac.cn (X. Li), hbdeng@whu.edu.cn, alphabeita@yahoo.com (H. Deng).
[1] Co-first author with the same contribution to this work.

http://dx.doi.org/10.1016/j.carbpol.2014.10.064
0144-8617/

properties (Deng et al., 2011b). In the current research, the nanofibrous cellulose mats, selected as the template, can be obtained by completely hydrolyzing the electrospun CA mats in alkaline solution. Then LZ and pectin could be alternately deposited on the surface of the template by LBL self-assembly technique, subsequently.

CA, as a natural polysaccharide and an ideal raw material used in food packaging, can be easily fabricated by electrospinning and get nanofibrous mats with fine mechanical properties (Huang et al., 2012). The negatively charged cellulose nanofibrous mats hydrolyzed from electrospun CA nanofibrous mats in NaOH solutions were eco-friendly materials, and could be selected as ideal template because of their negatively charged surface, low fiber density and good water insolubility.

LZ is an enzyme which can damage the cell wall of bacteria by catalyzing hydrolysis of 1,4-β-glycosidic bond between *N*-acetylmuramic and *N*-acetyl-D-glucosamine (Vanderkelen et al., 2011). Recently, LZ played a more and more important role in packaging materials for food fresh keeping and developing biodegradable nanoparticles for drug delivery as template (Conte et al., 2008). The practical application of free lysozyme is limited because it is unstable and easily inactivated. Therefore, most researchers have paid attentions to its immobilization (Gemili, Yemenicioğlu, & Altınkaya, 2009).

Pectin is biocompatible, non-toxic, and anionic natural polysaccharide and can be extracted from cell wall of most higher plants (Zouambia, Moulai-Mostefa, & Krea, 2009). It consists of α-(1–4)-bond D-galacturonic acid units chemically, interrupted occasionally by α-(1–2)-bond (Günter & Ovodov, 2011; Ralet, Lerouge, & Quéméner, 2009). Pectin is known as product in the food industry due to its ability to form aqueous gels (Canteri-Schemin, Fertonani, Waszczynskyj, & Wosiacki, 2005). Moreover, characters of excellent biocompatibility, effective bacterial inhibition ability and biodegradability entitle pectin to be a novel polymer material, which is employed in pharmaceutical industry, health promotion and treatment. It has been used potentially as a carrier for drug delivery to the gastrointestinal tract, such as matrix tablets, gel beads, film-coated dose form (Fan et al., 2012; Liu, Fishman, & Hicks, 2007).

In this study, LZ/pectin bilayers coated cellulose mats with LBL multilayer structure for bacteria inhibition were prepared successfully by LBL self-assembly technique. Scanning electron microscope (SEM), X-ray photoelectron spectroscopy (XPS) and thermal gravimetric analysis (TGA) were involved in characterizing the obtained LBL structured nanofibrous mats. Additionally, bacterial inhibition test was performed to measure the bacterial inhibition ability of the composite mats.

2. Materials and methods

2.1. Materials

Cellulose acetate (CA, $Mn = 3 \times 10^4$ Da) and pectin (from citrus fruits) were supplied by Sigma Aldrich Co., USA. Lysozyme (LZ, activity 25,000 U/mg) was provided by Amresco Co., USA. Other chemical reagents used in this research were all of chemical grade without any purification. All aqueous solutions were prepared using purified water with a resistance of 18.2 MΩ cm. In addition, *Escherichia coli* (*E. coli*) and *Staphylococcus aureus* (*S. aureus*) were obtained from China Center for Type Culture Collection, Wuhan University (Wuhan, China). Agar powder was supplied by Wuhan Huashun Biological Technology Co., Ltd. (Wuhan, China). Beef Extract and Peptone were both supplied by Beijing Shuangxuan Microorganism Technology Co., (Beijing, China).

2.2. Fabrication of CA nanofibrous mats

CA nanofibrous mats were fabricated by electrospinning technique according to our previous report (Deng et al., 2011b). A 16 wt% CA solution was prepared by dissolving CA powder in acetone and DMAC (*N*,*N*-dimethylacetamide) blending solvent, and the weight ratio of acetone and DMAC was 2:1. The electrostatic spinning device contains a high voltage DC power supply (DW-p303-1ACD8, Tianjin DongWen high voltage power supply CO., Tianjin, China) and syringe pump (LSP02-1B, Baoding Precision Pump CO., LTD, China). The prepared solutions were filled into a 10 mL syringe with a metal needle (the inner diameter was 0.8 mm) and driven by syringe pump. The applied voltage was 16 kV, and the tip-to-collector distance was 15 cm. The velocity of syringe pump was 1 mL/h. The environmental temperature and relative humidity were maintained at 25 °C and 45%, respectively. The prepared nanofibrous mats were dried at 60 °C for 5 h under vacuum for further characterizations.

2.3. Formation of LBL structured multilayers on nanofibrous mats

CA nanofibrous mats were hydrolyzed in 0.05 mol/L NaOH solutions for seven days to obtain cellulose mats before LBL process. Then the LBL structured films were assembled on the surface of the cellulose nanofibrous mats by the alternate adsorption of positively charged LZ and negatively charged pectin, and the schematic of this process was shown in Fig. 1. LY solution was prepared in 0.1 mol/L phosphate buffer solution (pH 6.24) at 4 °C with gentle stirring for 12 h and the concentration was 1 mg/mL. And 1 mg/mL pectin solution was prepared in the purified water at room temperature and stirred for 12 h. The ionic strengths of LZ, pectin, and rinsing solutions were regulated by adding NaCl at the 0.1 M concentration. The method for fabricating LBL structured films on nanofibers was identical with our previous literatures (Deng et al., 2011b, 2010). First, cellulose nanofibrous mats were immersed into positively charged LZ solution for 20 min followed by 2 min of washing in three NaCl solutions baths and then were immersed into negatively charged pectin solution for 20 min followed by identical rinsing procedures. Here, cellulose-(LZ/pectin)$_n$ was used as a formula to label the LBL structured films coated mats, where n was the number of the LZ/pectin bilayers. When n equaled to 5.5 or 10.5, the outermost layer was LZ. All resultant samples were dried at 30 °C for 24 h in vacuum prior to the subsequent characterizations.

2.4. Characterizations

The surface morphology of the as-spun nanofibrous mats and LBL films coated cellulose mats were analyzed by scanning electron microscopy (SEM, JSM-6700F, JEOL Co., Ltd., Japan). The average diameter of nanofibers was measured by Image analyzer (Photoshop). To identify the surface elemental composition of the LBL films coatings, a Karato Axis Ultra Imaging X-ray photoelectron spectrometer (XPS, Kratos Co., UK) was carried out. Fourier transform infrared (FT-IR) spectra were determined by a Nicolet FT-IR 5700 spectrophotometer (Nicolet, Madison, USA). The ζ-potential analysis was recorded by using nano-25 zetasizer (Malven, England). The thermal properties of nanofibrous mats was determined by differential scanning calorimetry (DSC204 F1, Netzsch, Germany) which were heated up twice from 20 to 450 °C with a heating rate of 10 °C/min under nitrogen flow (20 mL/min) to remove the heat history and thermo-gravimetric analysis (TGA, Pyris 1 TGA, PerKinElmer, USA) was conducted with a temperature range of 20–500 °C.

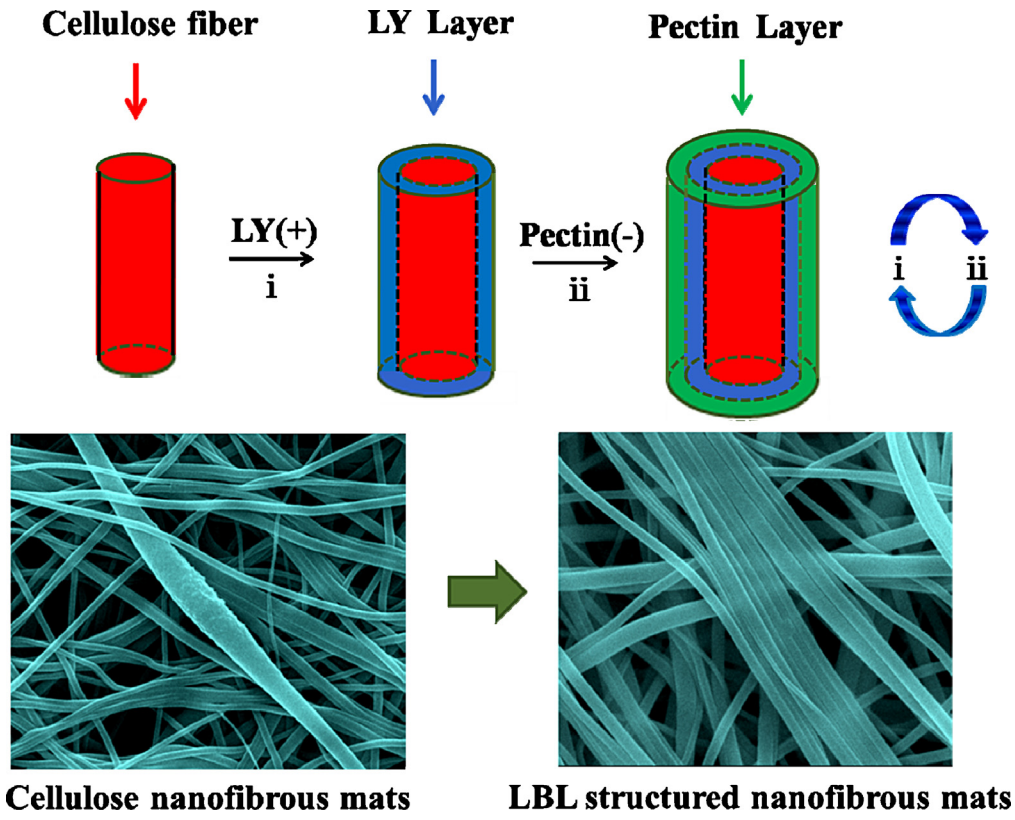

Fig. 1. Schematic of LBL modification process on nanofibrous mats.

2.5. Inhibition of bacterial ability

Disk-diffusion method was used for studying the bacterial inhibition activity of nanofibrous mats. Gram-positive *S. aureus* and Gram-negative *E. coli* were selected as representative microorganisms for investigation of antibacterial ability test, respectively. And manufactured bacterial suspensions were put into the thermostat shaker and incubated for 12 h. The nanofibrous mats were cut to disks with the diameter of 6 mm. Formulated meat-peptone broth were poured into a petri dish after high temperature and UV sterilization. For the antibacterial ability test, randomized five small nanofibrous mats were covered to a petri dish which has been coated with the bacteria suspension, and cultured at 37 °C for 12–15 h. Each sample was repeated for three times. The size of the zone around the nanofibrous mats was measured to characterize the inhibitory effect of the nanofibrous mats.

3. Results and discussion

3.1. Morphology analysis

As we know, the electrostatic deposition was the main driven force for electrostatic LBL modification. Table 1 shows ζ-potential values of cellulose and pectin are negatively charged, and the charge of LZ is +25 mV. Based on this fact, the positively charged LZ and negatively charge pectin could alternately deposited on the surface of negatively charged cellulose fibers through LBL self-assembly technique.

Table 1
ζ-Potential (mV) of cellulose fibrous mats, pectin and lysozyme.

Samples	Cellulose	Pectin	Lysozyme
ζ-Potential (mV)	−21.3	−26.0	+25.0

The SEM images were taken to observe the morphology of the as prepared mats (Fig. 2). Obviously, cellulose nanofibrous mats possessed very loosely packed cylindrical fibers in Fig. 2a. To study the impact of the number of coating bilayers on the formation of LBL films coated nanofibers, the cellulose nanofibers were coated with various numbers bilayers of LZ/pectin. The SEM images of cellulose fibers coated with various bilayers of LZ/pectin are shown in Fig. 2b–e. After the LBL films coated, the fibers tended to systematic align with each other and some parallel bundles of fibers could be observed among the mats, because the bilayers could adsorb the adjacent fibers and the solvent among the LBL films after evaporation could be split so that the fibers were slightly assembled together. The typically electrospun nanofibrous mats had a 3D structure with pores in micro scale before and after LBL modification. In general, there was no significant morphology difference between 5 and 5.5 bilayers coated mats, as well as 10 and 10.5 bilayers deposited mats (Deng et al., 2010). Besides, some junctions among the fibers were caused by the evaporation of the trace remained solvent during LBL process. In addition, the LBL films coatings presented slightly higher surface roughness on the surface of the fibers containing some irregular protuberances than the surface of the cellulose fibers, which caused by the inhomogenous LBL bilayers deposition (Huang et al., 2012). Different from other flat LBL templates, the deposition spaces among the adjacent fibers of mats were nonuniform and limited, resulting in the imbalance of the deposition driven force among the fibers. The deposition materials distributed or conglomerated in different sites, as the dispersion speed of deposition bilayers onto the cellulose mats was different. The average diameter of LBL films coated cellulose fibers was enlarged as the number of coating films increased. Based on the above results, the deposition of LZ and pectin could greatly affect the morphology of the LBL structured mats.

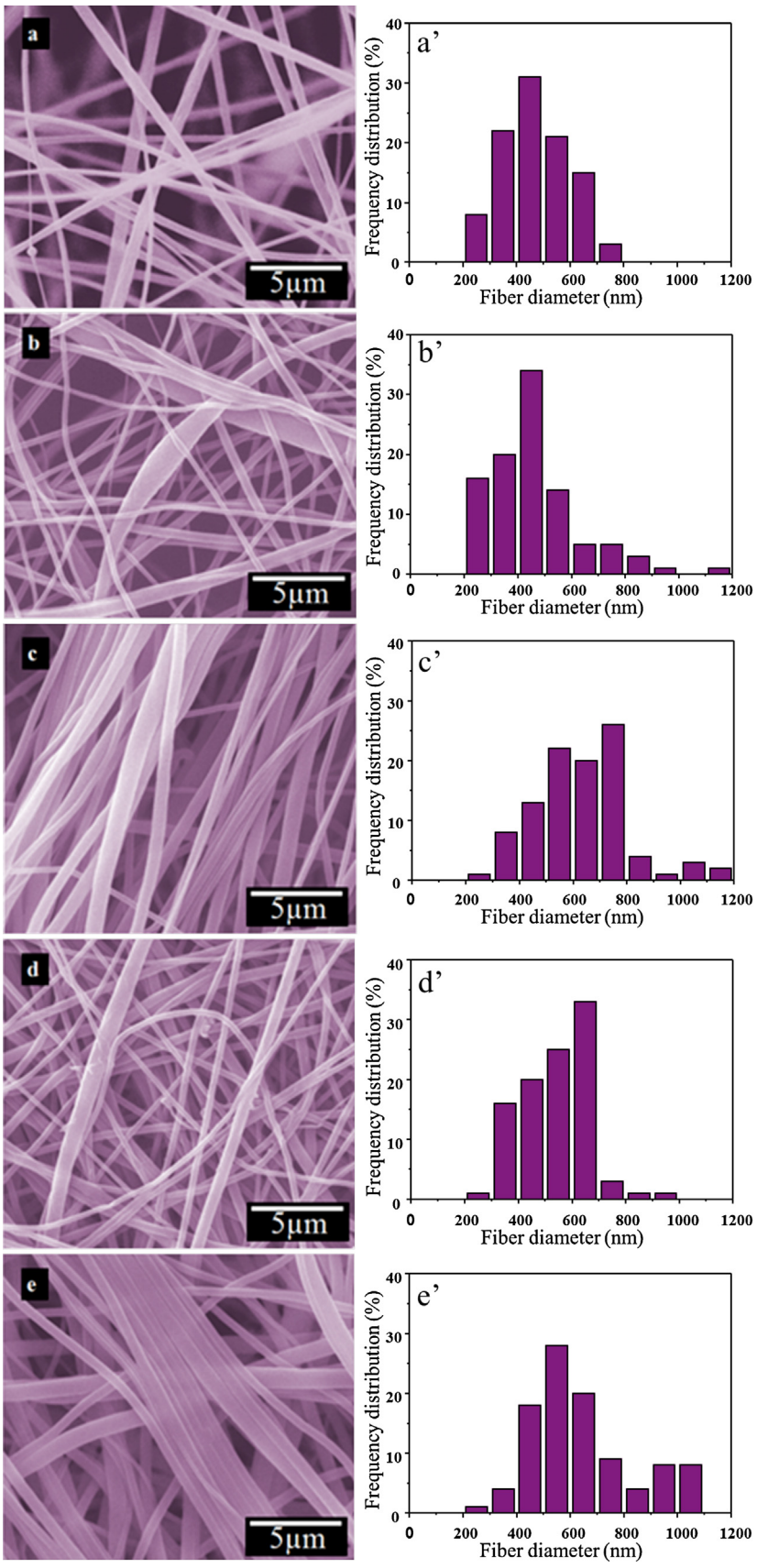

Fig. 2. SEM images of (a) cellulose nanofibrous mats and LBL structured nanofibrous mats coated with: (b) $(LZ/pectin)_5$, (c) $(LZ/pectin)_{5.5}$, (d) $(LZ/pectin)_{10}$ and (e) $(LZ/pectin)_{10.5}$. Images (a′)–(e′) show the fiber diameter distributions of (a)–(e), respectively.

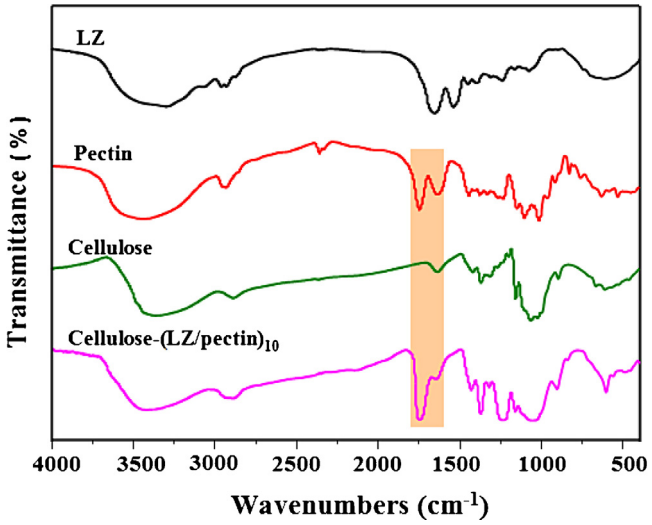

Fig. 3. FT-IR spectra of LZ powder, pectin powder, cellulose fibrous mats and $(LZ/pectin)_{10}$ films coated cellulose mats.

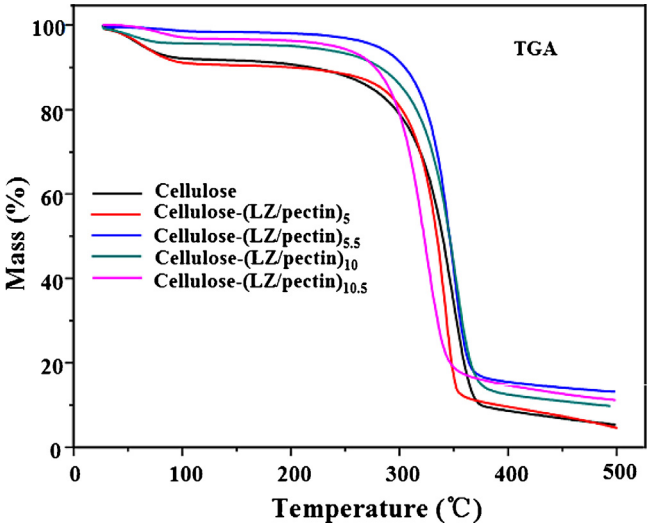

Fig. 5. TGA thermograms of: cellulose nanofibrous mats and LBL structured nanofibrous mats coated with $((LZ/pectin)_5$, $(LZ/pectin)_{5.5}$, $(LZ/pectin)_{10}$ and $(LZ/pectin)_{10.5}$.

3.2. FT-IR and XPS analysis

Fig. 3 shows FT-IR spectra of all component and composited mats. LZ had dominant bands at 1560 cm^{-1} and 1640 cm^{-1}, representing —NH and —C=O bending vibration (Blout, De Loze, & Asadourian, 1961; Hamill, Wang, & Lee, 2005), respectively. Pectin presented the absorption peaks at 1150 cm^{-1}, 1622 cm^{-1}, 1740 cm^{-1} and 2932 cm^{-1}, which were characteristics of the —CH—OH, —C=O, —C=O and —CH, respectively (Deng et al., 2011a). Besides, the absorption peak at 1556 cm^{-1} indicated —C=O stretching vibrations due to the presence of $—COOCH_3$ groups (Ranjha, Mudassir, & Sheikh, 2011). The cellulose nanofibrous mats exhibited an absorption peak at 1640 cm^{-1} which was attributed to carboxylic acid groups (—C—O—O) (Deng et al., 2010).

After the deposition of $(LZ/pectin)_{10}$ films on the surface of cellulose nanofibrous mats, the band of cellulose around 1740 cm^{-1} became broader, and the $(LZ/pectin)_{10}$ coated cellulose mats had a peak which was most likely attributable to the vibrational mode of carbonyl group (—C=O) from pectin. And the peak of LZ coincided with cellulose and $(LZ/pectin)_{10}$ coated cellulose mats at 1640 cm^{-1}, so the peak could not be attributed to any component. Hence, pectin has been successfully assembled onto the surface of the cellulose nanofibrous mats.

For further investigating whether LZ has been deposited successfully on the mats or not, XPS scans were performed to characterize the composition on the surface of the LBL films coated mats. Fig. 4 displays the XPS results of cellulose, $(LZ/pectin)_5$ films coated mats and $(LZ/pectin)_{10.5}$ films coated mats. It was known that the characteristic of pectin and cellulose were carbon, hydrogen, and oxygen elements. In Fig. 4a, Nitrogen could be detected, which confirmed that LZ was on the surface of the composited mats, including $(LZ/pectin)_5$ and $(LZ/pectin)_{10.5}$ films coated cellulose mats. The former was with pectin on the outmost layer and the later was with LZ on the outmost layer. Both of $(LZ/pectin)_5$ and $(LZ/pectin)_{10.5}$ films contained LZ. Besides, in Fig. 4b, nitrogen

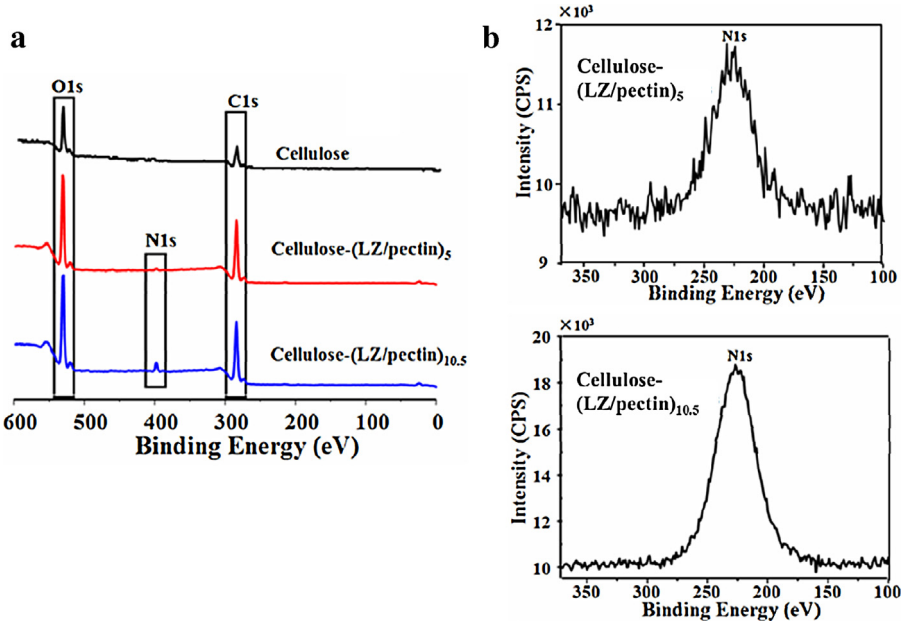

Fig. 4. XPS peak fitting curves of: (a) cellulose, $(LZ/pectin)_5$ films coated cellulose mats and $(LZ/pectin)_{10.5}$ films coated cellulose mats; (b) N 1s narrow scans.

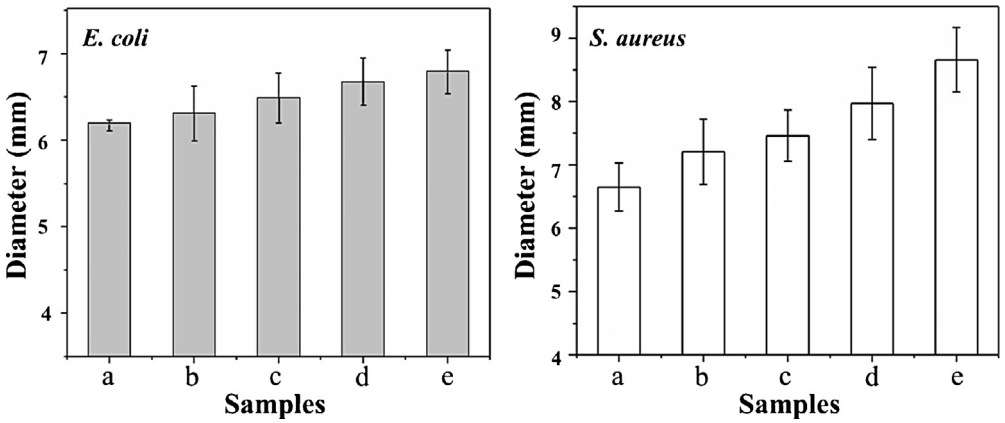

Fig. 6. Average diameters of bacterial growth inhibition zone against *E. coli* and *S. aureus* of: (a) cellulose nanofibrous mats and LBL structured nanofibrous mats coated with (b) $(LZ/pectin)_5$, (c) $(LZ/pectin)_{5.5}$, (d) $(LZ/pectin)_{10}$ and (e) $(LZ/pectin)_{10.5}$.

were found at 401.85 eV in the $(LZ/pectin)_5$ and $(LZ/pectin)_{10.5}$ films coatings with the percentage of 1.04% and 4.51%, respectively. The quantity of LZ was increased with increasing the numbers of coating bilayers. XPS results indicated that LZ has been successfully deposited.

3.3. Thermal properties analysis

The thermal stability of cellulose mats and the LBL films coated mats was evaluated by TGA analysis (Fig. 5). In fact, the structure, molecular weight, and conformation of the polymer played important roles in improving the properties of LBL structured mats. The T_{max} of all LBL structured mats were slightly higher than that of cellulose mats, and T_{max} of the LBL film-coatings with pectin in the outermost layer was slightly lower than those of the LBL film-coatings with LZ in the outermost layer. Here, T_{max} was the temperature when the rate of weight loss reached a maximum, which indicated the mass losses of cellulose-$(LZ/pectin)_n$ films were less than that of cellulose mats. This phenomenon indicated that the 3D structured cellulose-$(LZ/pectin)_n$ mats exhibited better thermal stability than pure cellulose mats. The presence of LZ/pectin in the cellulose mats with high aspect ratio acted as barriers, which might strongly hinder the out diffusion of the volatile decomposition products obtained from pyrolysis, as a direct result of the decrease in permeability. Besides, the fractional free volume of the LBL films coated mats became smaller so the intramolecular mobility of cellulose-$(LZ/pectin)_n$ mats was weakened. Therefore, it could be concluded that the LBL structured mats played a role in improving the thermal properties of the composite mats.

3.4. Bacterial inhibition results

Bacterial inhibition activity of the uncoated and LBL films coated mats against *S. aureus* and *E. coli* was investigated by inhibition zone surrounding circular mats disks (Fig. 6). Obviously, the cellulose nanofibrous mats showed little inhibitory effect, and the reason was that cellulose mats disks covered on the surface of the bacteria colonies could inhibit O_2 and CO_2 to contact with bacteria (Deng et al., 2012). In Fig. 6 the bacterial inhibition zone was enlarged when the number of coating films increased, as the numbers of bilayers was proportional to the quantity of antibacterial agents. The growth inhibition of $(LZ/pectin)_{10.5}$ films coated nanofibrous mats against the Gram-negative bacteria was 6.7 mm, while the growth inhibition of the Gram-positive bacteria was 8.6 mm. The results indicated that the addition of LZ/pectin could improve the antibacterial activity of the nanofibrous mats, and the antimicrobial activity of the samples with LZ in the outermost layer was better than that of the samples with pectin in the outermost layer. The reason was that LZ was positively charged and could absorb the negatively charged bacterial cells. Furthermore, LZ inhibited bacteria which can damage the cell walls of bacteria by catalyzing hydrolysis of 1,4-β-glycosidic bond between *N*-acetylmuramic acid and *N*-acetyl-D-glucosamine (Vanderkelen et al., 2011). The bacterial inhibition activity of the nanofibrous mats showed a weak inhibitory effect to the Gram-negative bacteria and the mats against Gram-positive bacteria was higher than that of the mats against the Gram-negative bacteria which might be caused by the reasons as follows: first, LZ showed antimicrobial activity on bacteria by attacking peptidoglycans (especially Gram-positive bacteria) and LZ is positively charged and could absorb the negatively charged bacterial cells, second, pectin showed bacterial inhibition activity by increasing viscosity and better property in Gram-positive bacterial inhibition than that in Gram-negative bacterial inhibition.

As a result, the self-assembly materials (LZ and pectin) was efficient to inhibit bacteria. The cellulose-$(LZ/pectin)_{10.5}$ LBL nanofibrous mats showed the best inhibitory effect among the prepared mats.

4. Conclusions

In this study, the nanofibrous cellulose mats hydrolyzed from the electrospun CA mats were chosen as template. LZ and pectin were alternately deposited on the template surface by LBL self-assembly technique to obtain antibacterial composite nanofibrous mats. SEM images showed that the average fiber diameter of the nanofibrous mats ranged from 406 nm to 537 nm. Besides, the FT-IR and XPS results confirmed that LZ and pectin were successfully adsorbed onto the surface of the nanofibers. The test of thermal properties showed that the LBL structure played a role in improving the thermal properties of the composite mats. The antibacterial assay results showed that the introduction of natural antibacterial agents LZ and pectin and the LBL multilayer structure resulted in enhanced bacterial inhibition activity.

Acknowledgements

This project was funded by the Major State Basic Research Development Program of China (973 Program, no. 2010CB732204) and National Natural Science Foundation of China (Nos. 31101365, 51473125 and 51303200).

References

Blout, E., De Loze, C., & Asadourian, A. (1961). The deuterium exchange of water-soluble polypeptides and proteins as measured by infrared spectroscopy. *Journal of the American Chemical Society*, *83*(8), 1895–1900.

Canteri-Schemin, M. H., Fertonani, H. C. R., Waszczynskyj, N., & Wosiacki, G. (2005). Extraction of pectin from apple pomace. *Brazilian Archives of Biology and Technology*, *48*(2), 259–266.

Conte, A., Buonocore, G., Sinigaglia, M., Lopez, L., Favia, P., d'Agostino, R., et al. (2008). Antimicrobial activity of immobilized lysozyme on plasma-treated polyethylene films. *Journal of Food Protection®*, *71*(1), 119–125.

Decher, G., Hong, J., & Schmitt, J. (1992). Buildup of ultrathin multilayer films by a self-assembly process: III. Consecutively alternating adsorption of anionic and cationic polyelectrolytes on charged surfaces. *Thin Solid Films*, *210*, 831–835.

Deng, H., Li, X., Ding, B., Du, Y., Li, G., Yang, J., et al. (2011). Fabrication of polymer/layered silicate intercalated nanofibrous mats and their bacterial inhibition activity. *Carbohydrate Polymers*, *83*(2), 973–978.

Deng, H., Lin, P., Li, W., Xin, S., Zhou, X., & Yang, J. (2013). Hydroxypropyl chitosan/organic rectorite-based nanofibrous mats with intercalated structure for bacterial inhibition. *Journal of Biomaterials Science, Polymer Edition*, *24*(4), 485–496.

Deng, H., Lin, P., Xin, S., Huang, R., Li, W., Du, Y., et al. (2012). Quaternized chitosan-layered silicate intercalated composites based nanofibrous mats and their antibacterial activity. *Carbohydrate Polymers*, *89*(2), 307–313.

Deng, H., Wang, X., Liu, P., Ding, B., Du, Y., Li, G., et al. (2011). Enhanced bacterial inhibition activity of layer-by-layer structured polysaccharide film-coated cellulose nanofibrous mats via addition of layered silicate. *Carbohydrate Polymers*, *83*(1), 239–245.

Deng, H., Zhou, X., Wang, X., Zhang, C., Ding, B., Zhang, Q., et al. (2010). Layer-by-layer structured polysaccharides film-coated cellulose nanofibrous mats for cell culture. *Carbohydrate Polymers*, *80*(2), 474–479.

Ding, J. H., & Gin, D. L. (2000). Catalytic Pd nanoparticles synthesized using a lyotropic liquid crystal polymer template. *Chemistry of Materials*, *12*(1), 22–24.

Fan, L., Cao, M., Gao, S., Wang, W., Peng, K., Tan, C., et al. (2012). Preparation and characterization of a quaternary ammonium derivative of pectin. *Carbohydrate Polymers*, *88*(2), 707–712.

Günter, Y. A., & Ovodov, Y. S. (2011). Pectin substances of the callus culture of *Silene vulgaris* (M.) G. *Applied Biochemistry and Microbiology*, *47*(1), 82–86.

Gemili, S., Yemenicioğlu, A., & Altınkaya, S. A. (2009). Development of cellulose acetate based antimicrobial food packaging materials for controlled release of lysozyme. *Journal of Food Engineering*, *90*(4), 453–462.

Hamill, A. C., Wang, S. C., & Lee, C. T. (2005). Probing lysozyme conformation with light reveals a new folding intermediate. *Biochemistry*, *44*(46), 15139–15149.

Hartgerink, J. D., Beniash, E., & Stupp, S. I. (2001). Self-assembly and mineralization of peptide-amphiphile nanofibers. *Science*, *294*(5547), 1684–1688.

Hou, Z., Li, C., Ma, P., Li, G., Cheng, Z., Peng, C., et al. (2011). Electrospinning preparation and drug-delivery properties of an up-conversion luminescent porous NaYF4: Yb3+, Er3 + @ silica fiber nanocomposite. *Advanced Functional Materials*, *21*(12), 2356–2365.

Huang, W., Xu, H., Xue, Y., Huang, R., Deng, H., & Pan, S. (2012). Layer-by-layer immobilization of lysozyme–chitosan–organic rectorite composites on electrospun nanofibrous mats for pork preservation. *Food Research International*, *48*(2), 784–791.

Liu, L., Fishman, M. L., & Hicks, K. B. (2007). Pectin in controlled drug delivery—A review. *Cellulose*, *14*(1), 15–24.

Marcus, J. S., Anderson, W. F., & Quake, S. R. (2006). Parallel picoliter RT-PCR assays using microfluidics. *Analytical Chemistry*, *78*(3), 956–958.

Noh, H. K., Lee, S. W., Kim, J.-M., Oh, J.-E., Kim, K.-H., Chung, C.-P., et al. (2006). Electrospinning of chitin nanofibers: Degradation behavior and cellular response to normal human keratinocytes and fibroblasts. *Biomaterials*, *27*(21), 3934–3944.

Ralet, M.-C., Lerouge, P., & Quéméner, B. (2009). Mass spectrometry for pectin structure analysis. *Carbohydrate Research*, *344*(14), 1798–1807.

Ranjha, N. M., Mudassir, J., & Sheikh, Z. Z. (2011). Synthesis and characterization of pH-sensitive pectin/acrylic acid hydrogels for verapamil release study. *Iranian Polymer Journal*, *20*(2), 147–159.

Vanderkelen, L., Van Herreweghe, J., Vanoirbeek, K., Baggerman, G., Myrnes, B., Declerck, P., et al. (2011). Identification of a bacterial inhibitor against g-type lysozyme. *Cellular and Molecular Life Sciences*, *68*(6), 1053–1064.

Wang, X., Ding, B., Yu, J., Si, Y., Yang, S., & Sun, G. (2011). Electro-netting: Fabrication of two-dimensional nano-nets for highly sensitive trimethylamine sensing. *Nanoscale*, *3*(3), 911–915.

Yang, X., Chen, X., & Wang, H. (2009). Acceleration of osteogenic differentiation of preosteoblastic cells by chitosan containing nanofibrous scaffolds. *Biomacromolecules*, *10*(10), 2772–2778.

Yu, H., Yu, J., Liu, S., & Mann, S. (2007). Template-free hydrothermal synthesis of CuO/Cu_2O composite hollow microspheres. *Chemistry of Materials*, *19*(17), 4327–4334.

Zhang, Y., Venugopal, J., Huang, Z.-M., Lim, C., & Ramakrishna, S. (2005). Characterization of the surface biocompatibility of the electrospun PCL-collagen nanofibers using fibroblasts. *Biomacromolecules*, *6*(5), 2583–2589.

Zouambia, Y., Moulai-Mostefa, N., & Krea, M. (2009). Structural characterization and surface activity of hydrophobically functionalized extracted pectins. *Carbohydrate Polymers*, *78*(4), 841–846.